Supporting Information

Synthetic strategy for graphitized carbon hollow nanospheres with nano-punched hole decorated with bimetallic selenide as efficient bifunctional electrocatalysts for rechargeable Li-O_2 batteries

Jeong Hoo Hong,[a] Jin Koo Kim,[a] Dae Soo Jung,[*b] and Yun Chan Kang[*a]

[a]Department of Materials Science and Engineering, Korea University, 145 Anam-ro, Seongbuk-gu, Seoul 02841, Republic of Korea

[b]Energy and Environment Division, Korea Institute of Ceramic Engineering and Technology (KICET), Jinju, Gyeongnam 52851, Republic of Korea

* Corresponding author:

E-mail address: yckang@korea.ac.kr; (Yun Chan Kang), dsjung@kicet.re.kr; (Dae Soo Jung)

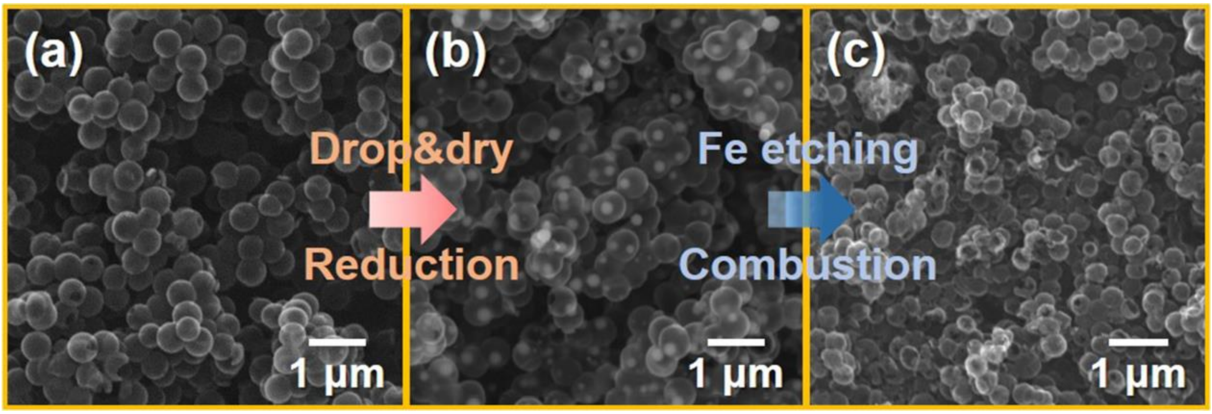

Fig. S1. SEM images of (a) PAH, (b) Fe@graphitic/amorphous carbon composite hollow nanospheres, and (c) PGH.

Table S1. The resistive properties of PGH and PAH.

Prepared sample	PGH	PAH
Resistivity (kOhm sq^{-1})	4.521	26.82

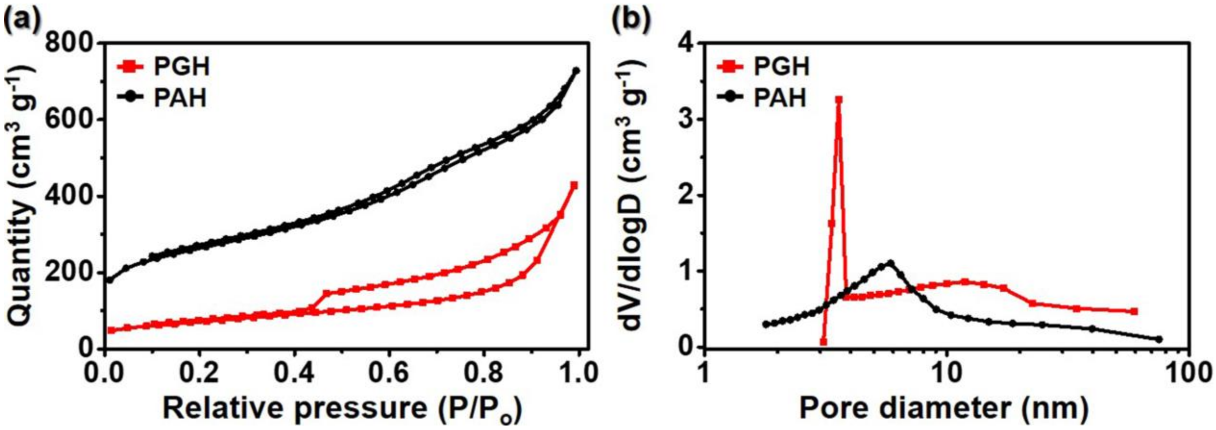

Fig. S2. (a) N_2 gas adsorption and desorption isotherms and (b) pore size distributions of PGH and PAH.

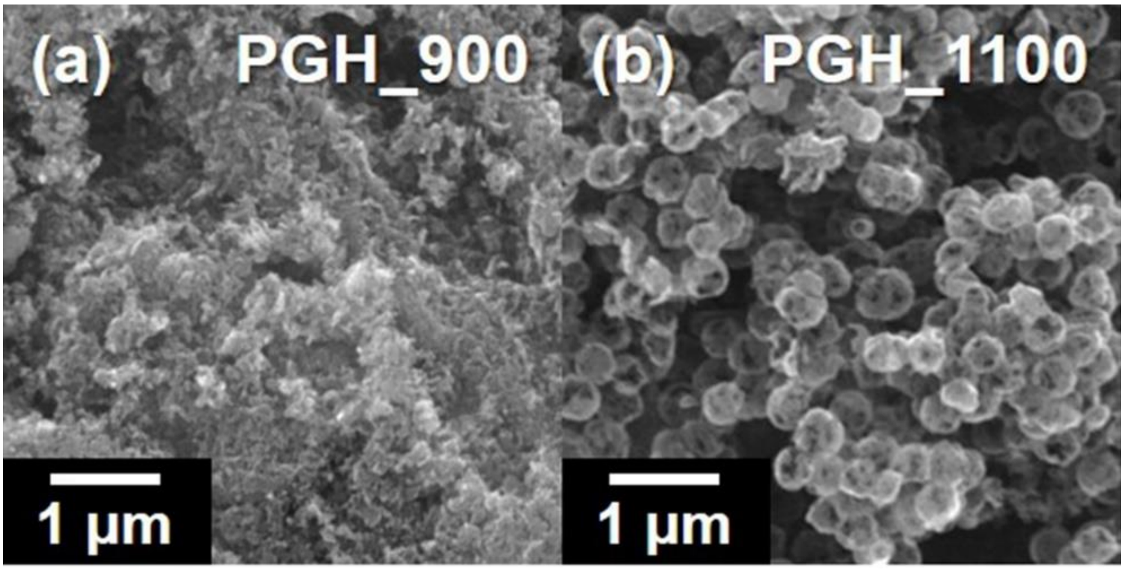

Fig. S3. SEM images of (a) PGH_900 and (b) PGH_1100.

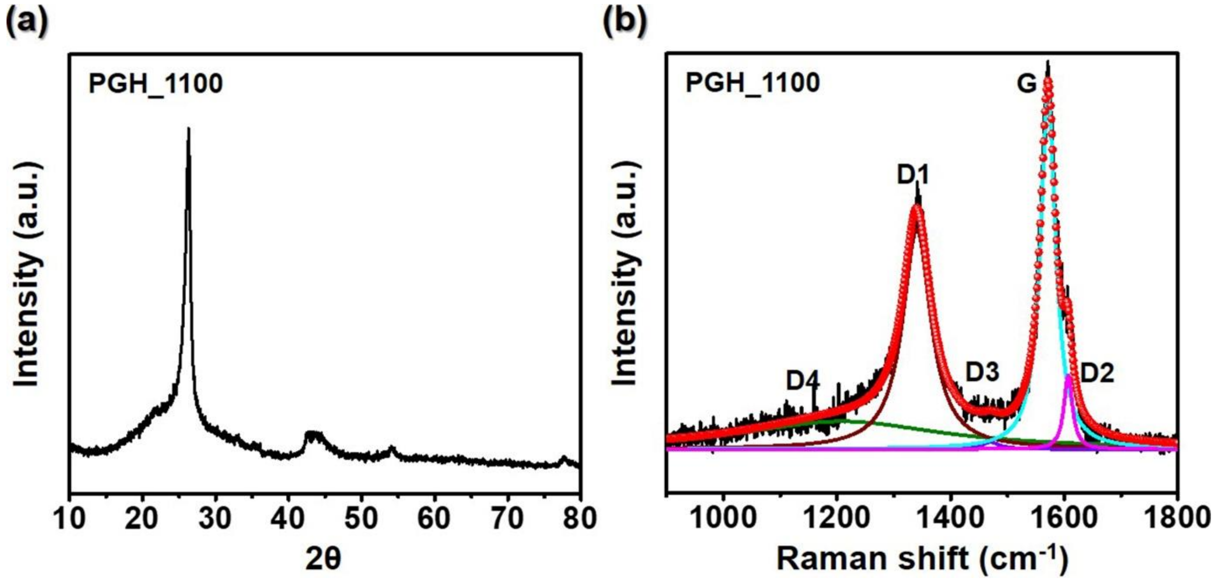

Fig. S4. (a) XRD pattern and (b) fitted Raman spectrum of PGH_1100.

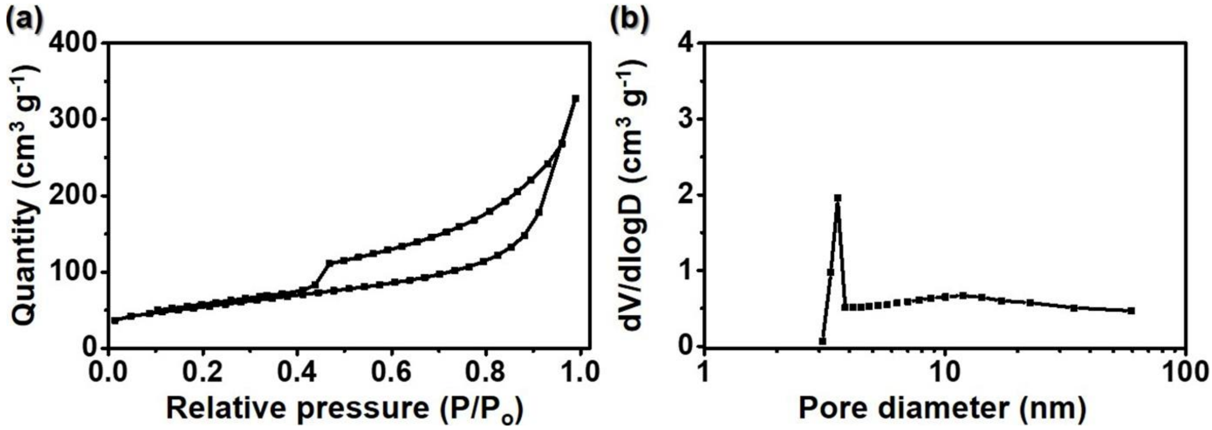

Fig. S5. (a) N_2 gas adsorption and desorption isotherm and (b) pore size distribution of PGH_1100.

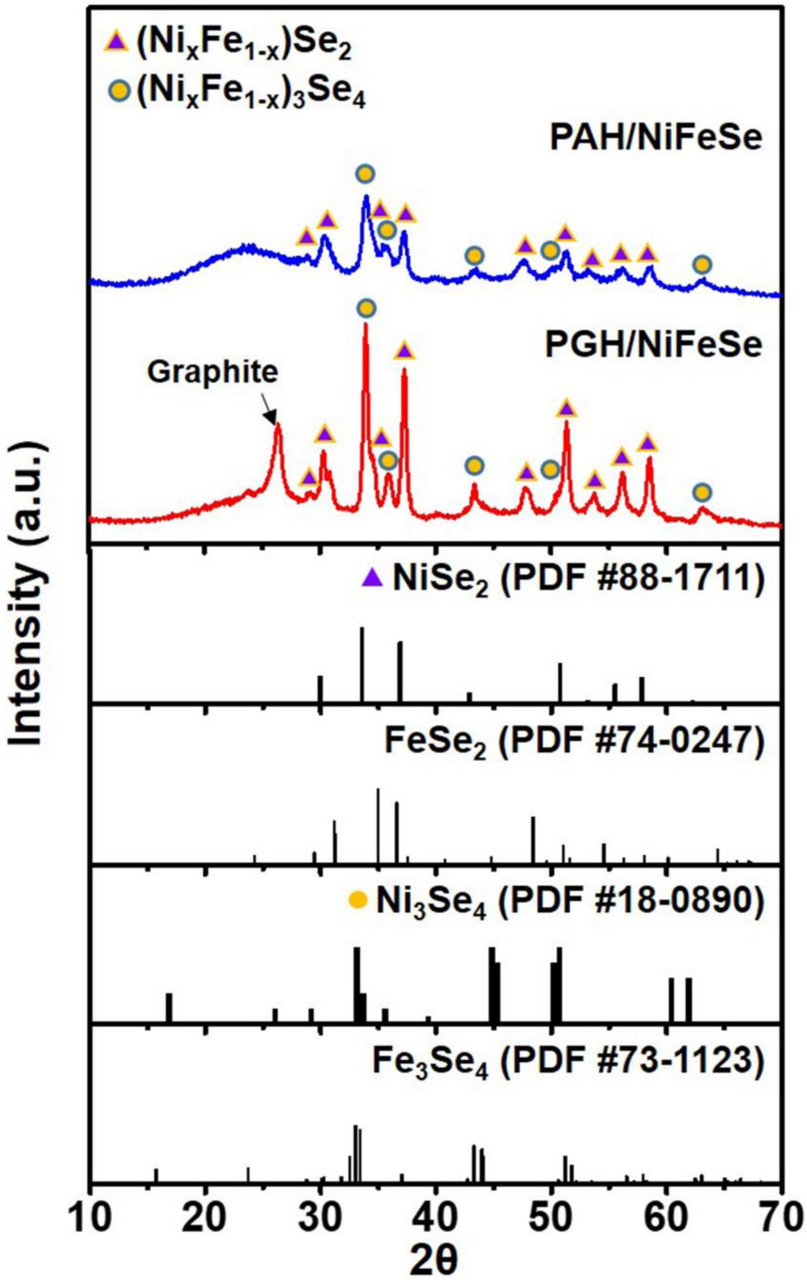

Fig. S6. XRD patterns of PAH/NiFeSe and PGH/NiFeSe.

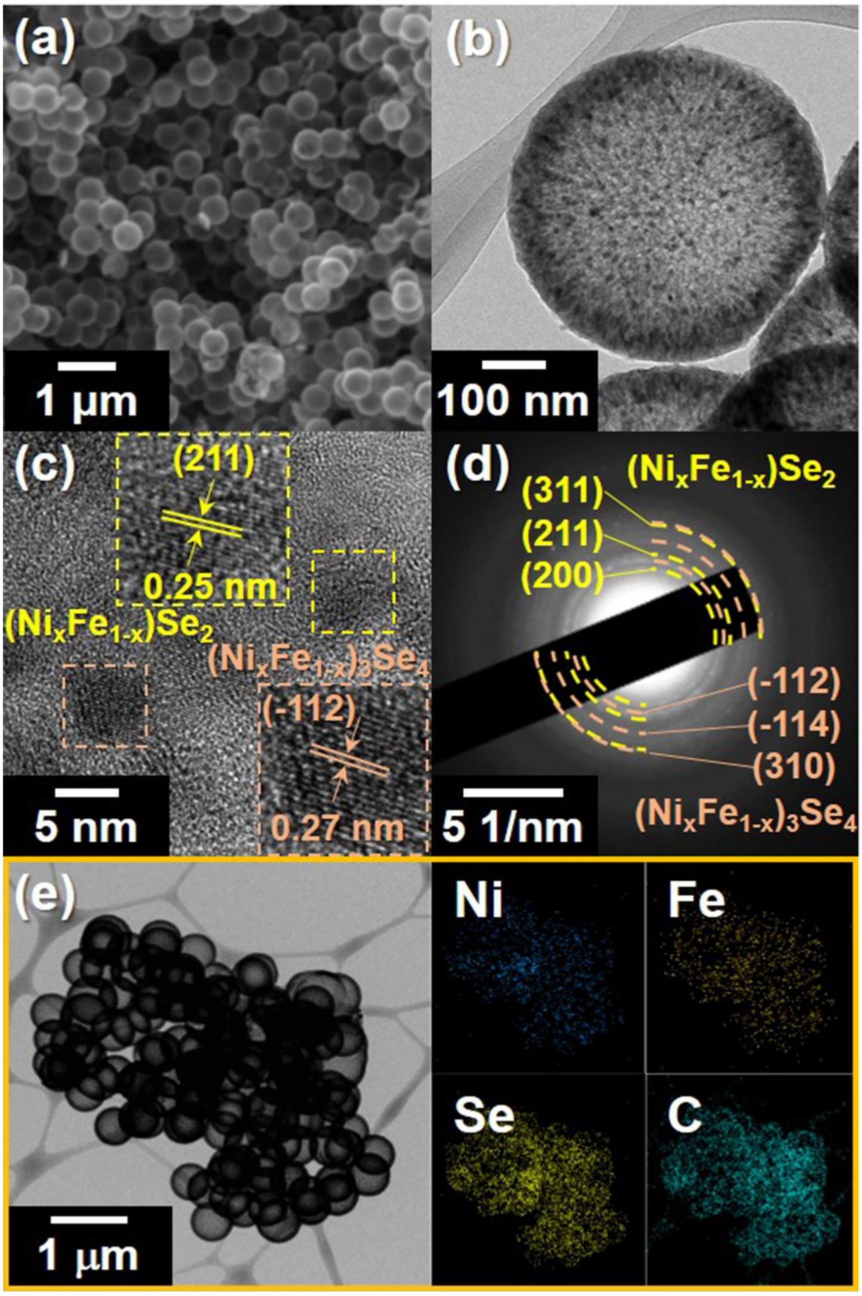

Fig. S7. Morphologies, SAED pattern, and elemental mapping images of PAH/NiFeSe: (a) SEM image, (b) TEM image, (c) HR-TEM image, (d) SAED pattern, and (e) elemental mapping images.

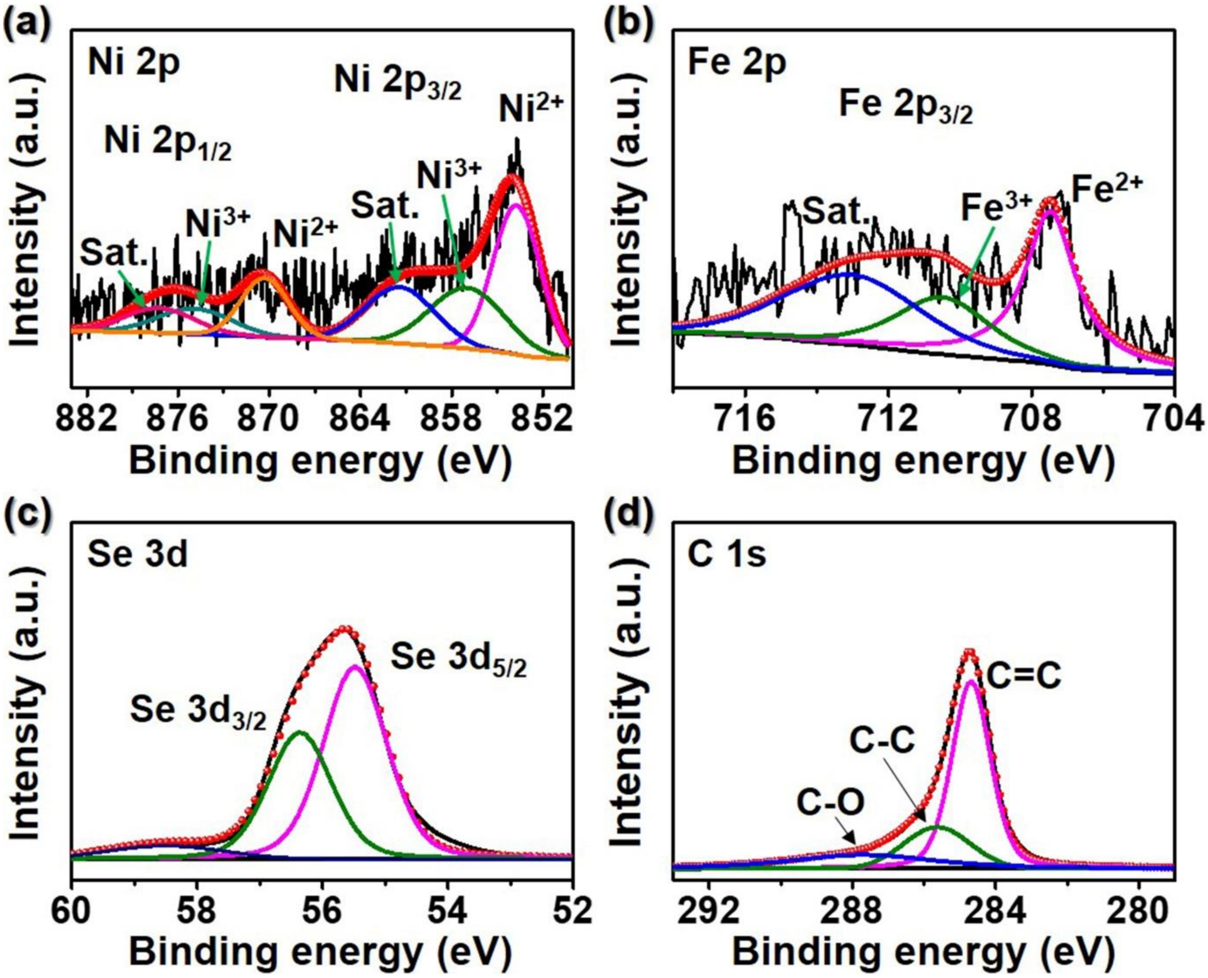

Fig. S8. XPS spectra of PAH/NiFeSe: (a) Ni 2p, (b) Fe 2p, (c) Se 3d, and (d) C 1s.

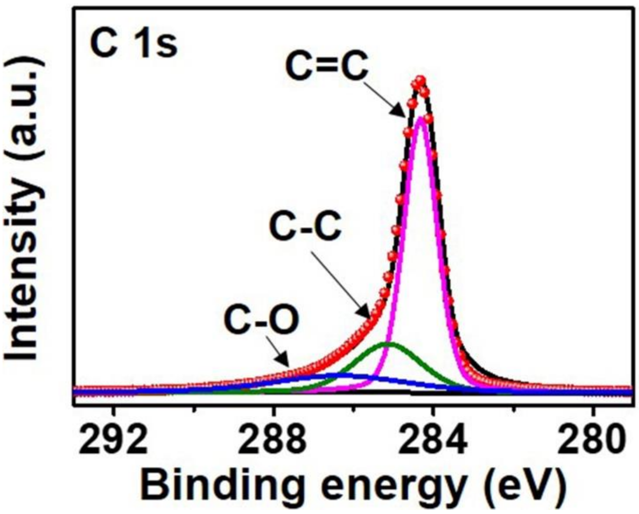

Fig. S9. C 1s spectrum of PGH.

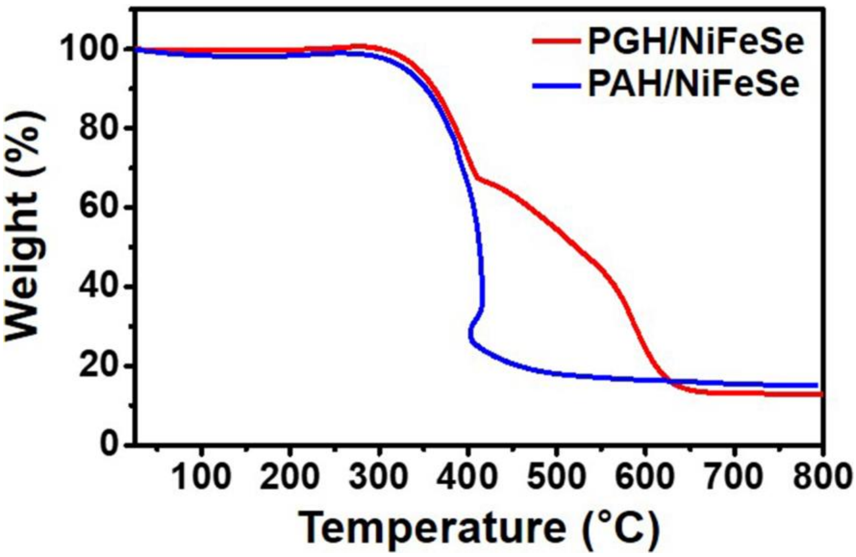

Fig. S10. TG curves of PGH/NiFeSe and PAH/NiFeSe.

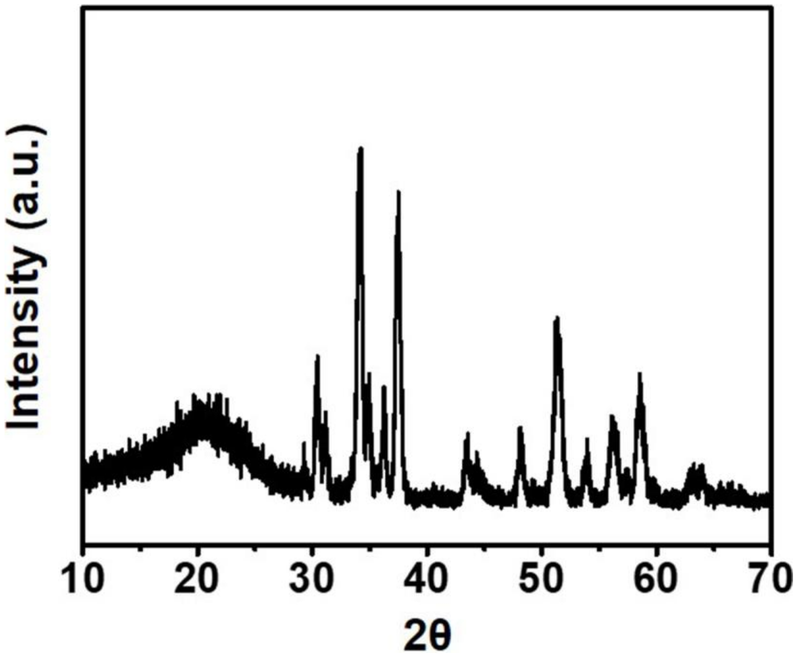

Fig. S11. XRD pattern of b-NiFeSe.

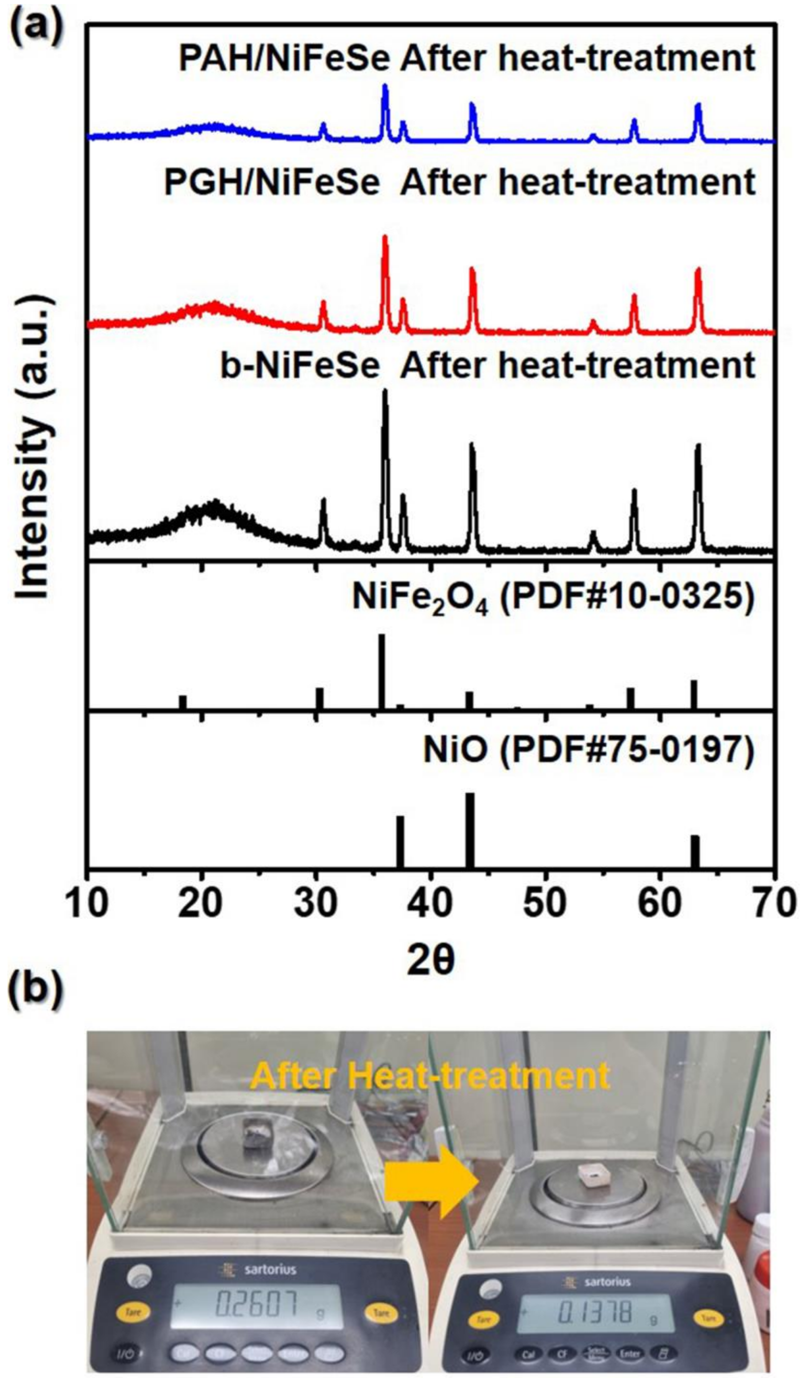

Fig. S12. (a) XRD patterns of PAH/NiFeSe, PGH/NiFeSe, and b-NiFeSe after heat-treatment under the same conditions as those used for TGA and (b) weight change of b-NiFeSe before and after heat-treatment.

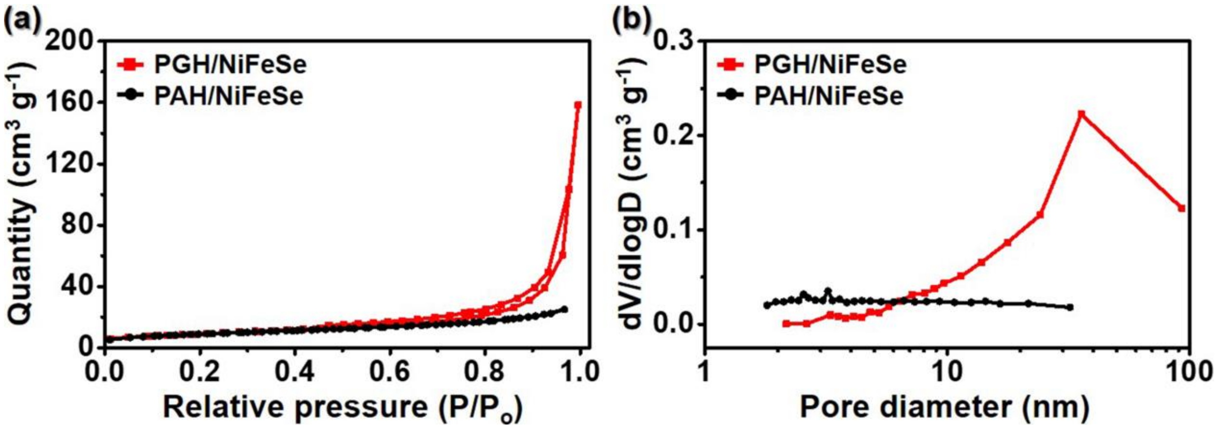

Fig. S13. (a) N_2 gas adsorption and desorption isotherms and (b) pore size distributions of PGH/NiFeSe and PAH/NiFeSe.

Table S2. Electrocatalytic properties of various transition metal selenide-based cathode for Li-O_2 batteries reported in the previous studies.

Sample	**Loading mass (mg cm^{-2})**	**Overpotential (V)**	**Discharge capacity (mA h g^{-1})**	**Ref**
Sisal-like $CoSe_2$ nanowires enriched with Se vacancies anchored on N-doped carbon cloth	N/A	0.81	6,089 (100 mA g^{-1})	[S1]
$CoSe_2$@$NiSe_2$ heterostructure with distinct heterogeneous interfaces	N/A	0.77	3,530 (600 mA g^{-1})	[S2]
SnSe nanosheets with exposed 2D surface (200) facets and stack edge facets	0.4	0.77	6,405 (2,000 mA g^{-1})	[S3]
Ni_3Se_2/$NiSe_2$ heterostructure nanoforests	N/A	0.96	23,092 (500 mA g^{-1})	[S4]
FeSe hollow spheroids	0.35	0.91	14,273 (500 mA g^{-1})	[S5]
Se vacancy rich NiSe nanorods on the Ni foam framework	N/A	0.58	5,412 (100 mA g^{-1})	[S6]
NiS_2/$NiSe_2$ homologous heterostructure	N/A	1.58	18,408 (100 mA g^{-1})	[S7]
$NiSe_2$@NiO heterogeneous structures on carbon cloth	N/A	0.3	11,512 (500 mA g^{-1})	[S8]
PGH/NiFeSe	0.5	0.61	18,596 (2,000 mA g^{-1})	This work

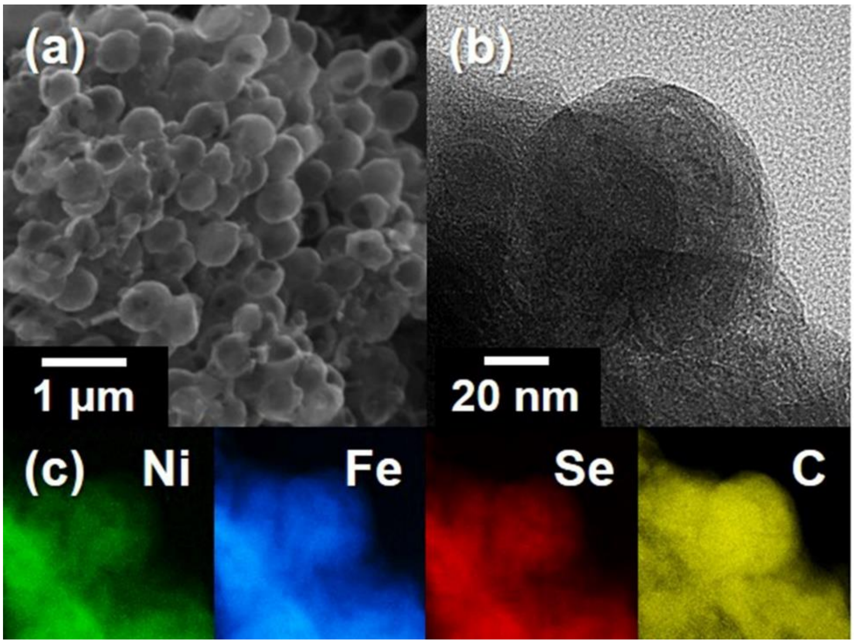

Fig. S14. (a) SEM image, (b) TEM image, and (c) elemental mapping images of PGH/NiFeSe after cycling stability test.

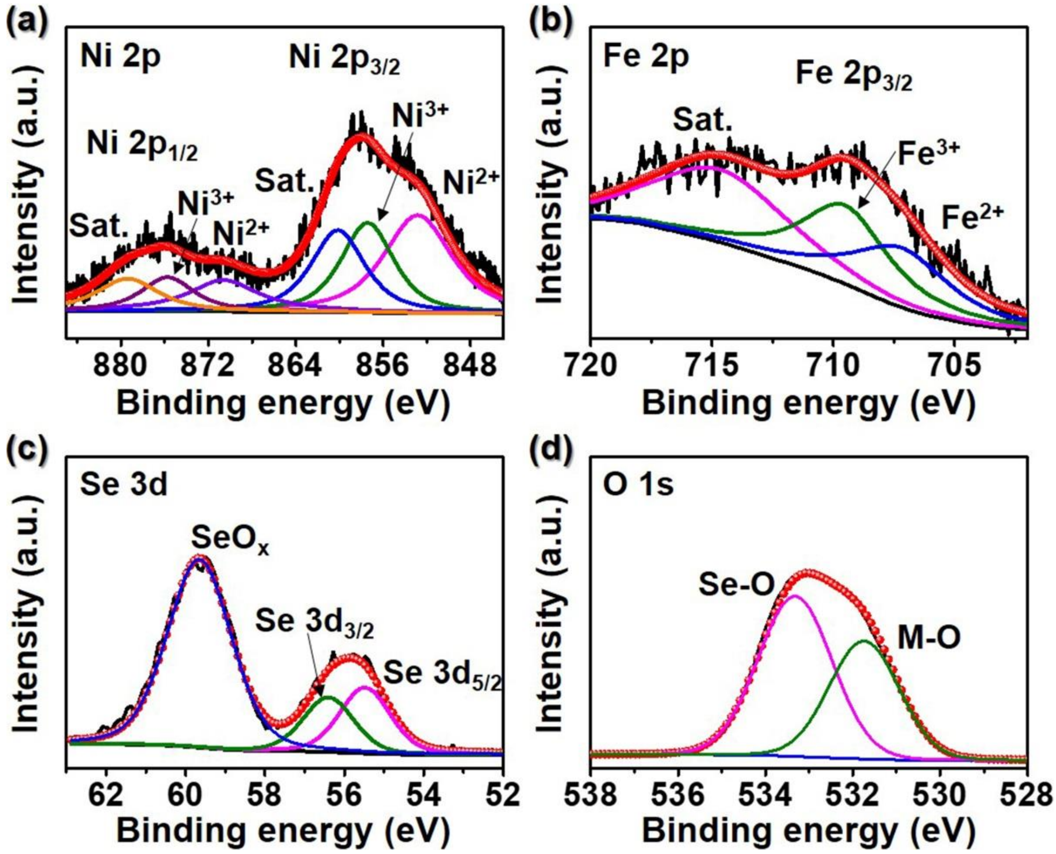

Fig. S15. XPS spectra of PGH/NiFeSe after cycling stability test: (a) Ni 2p, (b) Fe 2p, (c) Se 3d, and (d) O 1s.

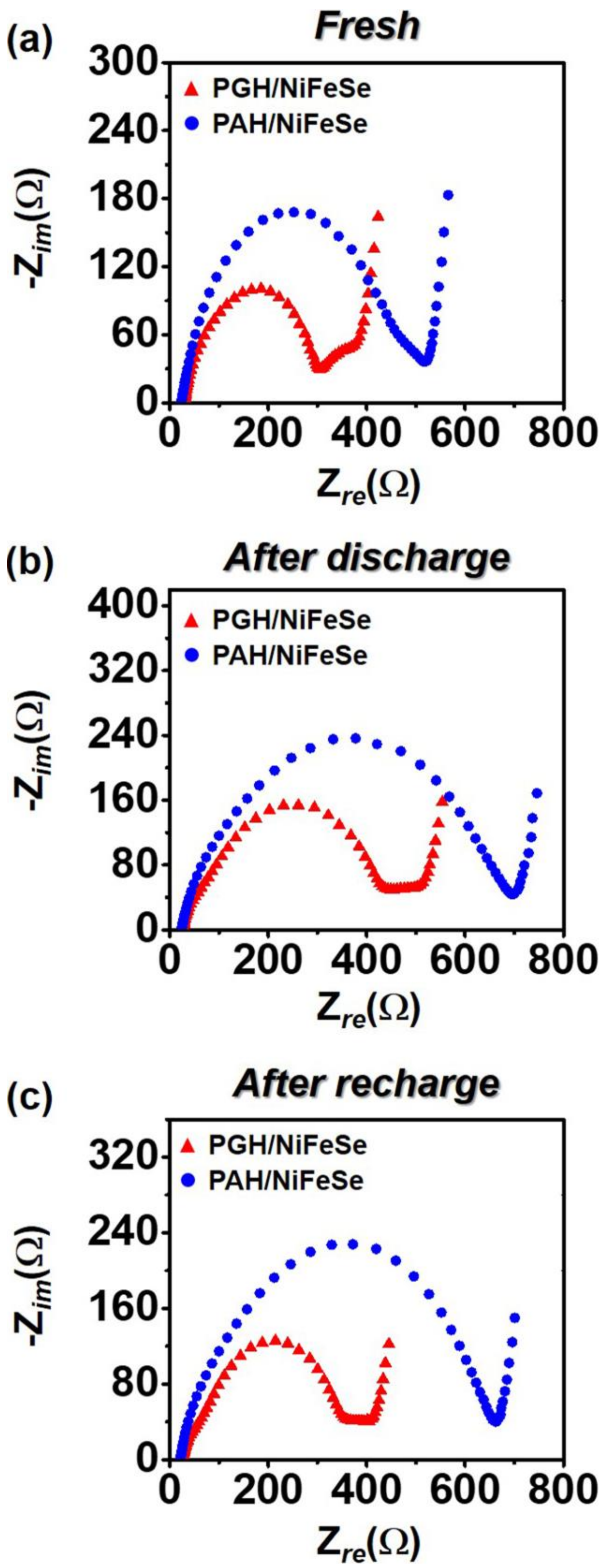

Fig. S16. Nyquist plots of PGH/NiFeSe and PAH/NiFeSe: (a) Fresh state, (b) after 1st discharge process, and (c) after 1st recharge process.

References

[S1] Z. Hou, C. Shu, R. Zheng, C. Liu, Z. Ran, T. Yang, P. Hei, Q. Zhang and J. Long, *J. Mater. Chem. A*, 2020, **8**, 16636-16648.

[S2] R. Liang, C. Shu, A. Hu, M. Li, Z. Ran, R. Zheng and J. Long, *Chem. Eng. J.*, 2020, **393**, 124592.

[S3] G. Zhang, G. Li, J. Wang, H. Tong, J. Wang, Y. Du, S. Sun and F. Dang, *Adv. Energy Mater.*, 2022, **12**, 2103910.

[S4] Z. Ran, C. Shu, Z. Hou, L. Cao, R. Liang, J. Li, P. Hei, T. Yang and J. Long, *J. Power Sources*, 2020, **468**, 228308.

[S5] H. Yoo, G.-H. Lee and D.-W. Kim, *J. Alloys Compd.*, 2021, **856**, 158269.

[S6] Z. Hou, P. Hei, C. Shu, R. Zheng, T. Yang, Q. Zhang and J. Long, *ACS Sustainable Chem. Eng.*, 2020, **8**, 6667-6674.

[S7] X. Han, L. Zhao, Y. Liang, J. Wang, Y. Long, Z. Zhou, Y. Zhang, Y. Li and J. Ma, *Adv. Energy Mater.*, 2022, 2202747.

[S8] X. Wen, Z. Ran, R. Zheng, D. Du, C. Zhao, R. Li, H. Xu, T. Zeng and C. Shu, *J. Alloys Compd.*, 2022, **901**, 163703.